

# Barrier Island Reconfiguration Leads to Rapid Erosion and Relocation of a Rural Alaska Community

Richard M. Buzard<sup>†\*</sup>, Nicole E.M. Kinsman<sup>‡</sup>, Christopher V. Maio<sup>†</sup>, Li H. Erikson<sup>§</sup>, Benjamin M. Jones<sup>††</sup>, Scott Anderson<sup>†††</sup>, Roberta J.T. Glenn<sup>†</sup>, and Jacquelyn R. Overbeck<sup>§§</sup>

<sup>†</sup>Department of Geosciences  
University of Alaska Fairbanks  
Fairbanks, AK 99775, U.S.A.

<sup>§</sup>U.S. Geological Survey  
Pacific Coastal and Marine Science Center  
Santa Cruz, CA 95060, U.S.A.

<sup>††</sup>Native Village of Port Heiden  
Port Heiden, AK 99549, U.S.A.

<sup>‡</sup>National Geodetic Survey  
National Oceanic and Atmospheric Administration  
Anchorage, AK 99513, U.S.A.

<sup>†††</sup>Institute of Northern Engineering  
University of Alaska Fairbanks  
Fairbanks, AK 99775, U.S.A.

<sup>§§</sup>Alaska Division of Geological & Geophysical Surveys  
Anchorage, AK 99508, U.S.A.



www.cerf-jcr.org

## ABSTRACT



www.JCRonline.org

Buzard, R.M.; Kinsman, N.E.M.; Maio, C.V.; Erikson, L.H.; Jones, B.M.; Anderson, S.; Glenn, R.J.T., and Overbeck, J.R., 0000. Barrier island reconfiguration leads to rapid erosion and relocation of a rural Alaska community. *Journal of Coastal Research*, 00(0), 000-000. Charlotte (North Carolina), ISSN 0749-0208.

Coastal erosion is one of the foremost hazards that circumpolar communities face. Climate change and warming temperatures are anticipated to accelerate coastal change, increasing risk to coastal communities. Most erosion hazard studies for Alaska communities only consider linear erosion and do not anticipate coastal morphologic changes. This study showcases the possibility and consequence of accelerated erosion by examining a shift from stability to rapid erosion that forced the rural Alaska Native village of Meshik (now Port Heiden) to abandon the original town site and relocate inland. A combination of remote sensing, coastal surveys, and community-based monitoring are used to map coastal morphologic changes and identify erosion drivers. The community's shoreline was stable until a protective barrier island eroded away. The exposure to open ocean waves, coupled with unconsolidated, low-density sediments, led to rapid erosion rates averaging  $5.8 \pm 0.6$  m/y from the 1970s to 2020s. The sudden and rapid erosion put great stress on Meshik residents and resulted in the loss of homes, erosion of a safe boat harbor, and pollution of the beach and bay. Erosion of the barrier island coincided with a period of greater storm activity and sea ice decline, but the exact cause could not be determined. Many polar communities are built on or behind barriers and are on erodible soils such as sands and thawing permafrost. This study highlights the need to study, monitor, and predict morphologic change and regime shifts that can bring catastrophic impacts to coastal communities.

**ADDITIONAL INDEX WORDS:** *Coastal retreat, shoreline change, community relocation, barrier systems, significant wave height, storm surge, community-based monitoring.*

## INTRODUCTION

Coastal communities are threatened by a multitude of projected outcomes from climate change, including the reconfiguration of protective barrier systems (Irrgang *et al.*, 2022; Stutz and Pilkey, 2011). Coastal barrier systems, including islands and spits, are formed by waves depositing sediment. Barriers absorb wave energy, reducing storm surge and waves reaching the mainland. Globally, sea-level rise is expected to increase the prevalence of runaway barrier island transgression (FitzGerald *et al.*, 2018). In polar regions, where sea ice has declined rapidly, wave energy and associated coastal hazards are anticipated to increase (Fritz, Vonk, and Lantuit, 2017). Following sea ice decline, Alaska's barrier systems have become increasingly mobile (Farquharson *et al.*, 2018; Gibbs

and Richmond, 2015). Many Alaska communities experience erosion and flood hazards (Buzard *et al.*, 2021b,c), but several are protected by barrier islands and spits. To begin answering how coastal reconfiguration may affect communities, this study examines the impact of barrier deterioration for the Alaska Native village of Meshik.

Western and northern Alaska comprise the communities most affected by coastal hazards (Overbeck *et al.*, 2020). Most are Alaska Native villages in remote locations with relatively small populations. These communities often lack redundancies for communitywide critical infrastructure (*e.g.*, power and water treatment) and rely on subsistence practices to obtain food. These aspects bring specific vulnerabilities, allowing coastal storms the potential to cause communitywide disasters. For example, the September 2022 typhoon Merbok destroyed boats, fishing and hunting equipment, and food stocks for the community of Chevak, triggering food insecurity (Schwing, 2022). Several communities facing frequent and imminent hazards are pursuing mitigation or relocation (U.S. Government Accountability Office Staff, 2022). Although it appears

DOI: 10.2112/JCOASTRES-D-22-00093.1 received 7 October 2022; accepted in revision 10 January 2023; corrected proofs received 22 February 2023; published pre-print online 27 March 2023.

\*Corresponding author: rmbuzard@alaska.edu

©Coastal Education and Research Foundation, Inc. 2023

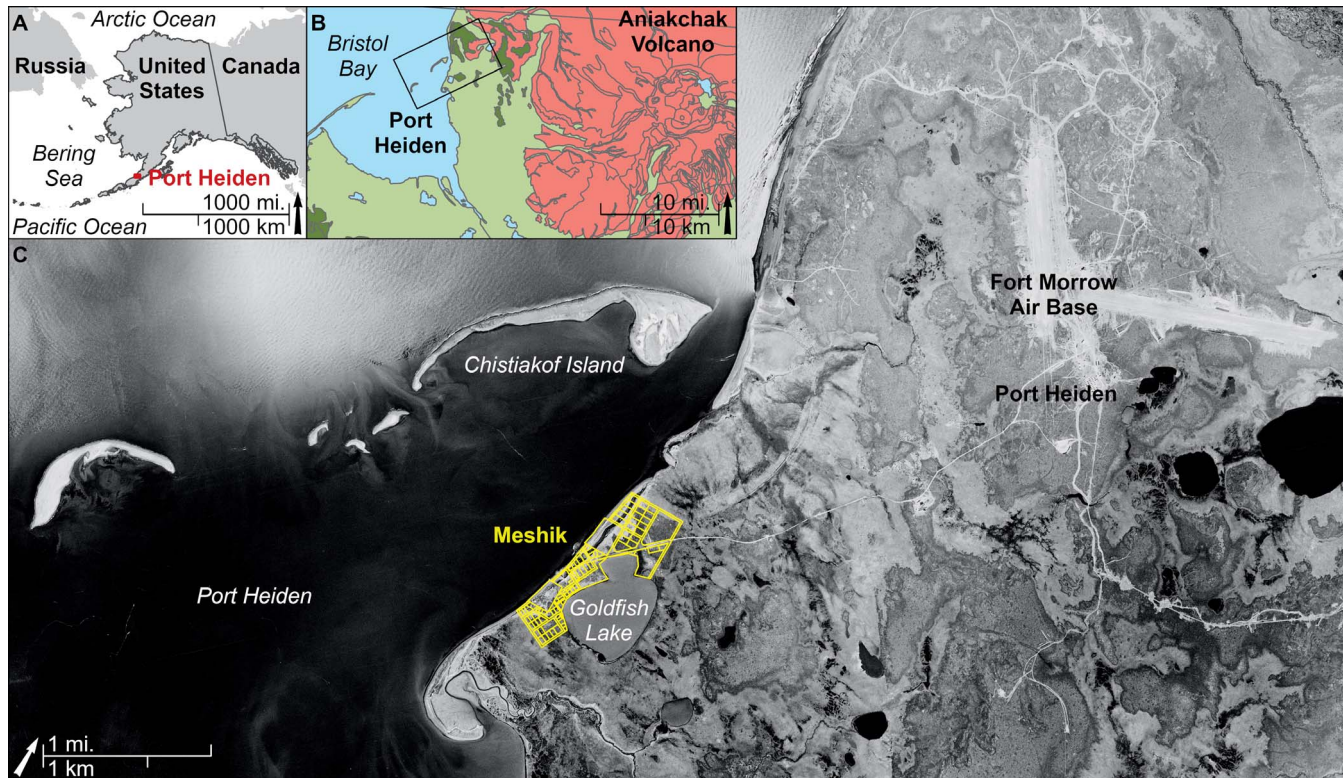


Figure 1. (A) Port Heiden is in SW Alaska, on the east shore of the Bering Sea. (B) Port Heiden is west of the Aniakchak volcano (igneous sediments in red). Most surficial geology consists of eolian or alluvium deposits (light green), with smaller areas of glacial sediments (dark green). (C) A 1957 image of the Meshik area (yellow) on the east shore of Port Heiden. A series of barrier islands existed, along with a channel along the coast that allowed southern alongshore currents to develop sand spits. The community eventually relocated along the road system south of the airport runways.

that hazardous events have risen significantly in these communities, it is more often the case that communities are built in hazard-prone areas (Buzard *et al.*, 2021b,c). For example, in the 1950s, Buckland's first school was built in a floodplain for convenient barge access (Alaska Rural Water and Sanitation Working Group, 2015). The community relocated from a nearby plateau into the floodplain to be near the school and experiences frequent flooding as a result. Bronen and Chapin (2013) detailed more examples of historically safe communities settling in hazard-prone areas. Hazard projections based on historical trends identify existing hazard-prone areas but could not identify the unprecedented hazards experienced by Meshik.

The focus of this study is to measure erosion and identify drivers of geomorphic change at the Alaska Native village of Meshik (Figure 1). Meshik was not in a hazard-prone area until the protective barrier island eroded away in the 1970s. After this, the mainland became one of the fastest-eroding shorelines in Alaska and the coastal community had to remove or abandon every structure, relocating inland to found the city of Port Heiden. By 2021, the former community footprint had entirely eroded away. This study investigates geologic and geomorphic parameters to develop a coastal evolution map, identifies the cause of rapid erosion, and compares environmental change and constants to discuss causal links. These results have

implications for coastal communities built on erodible soils and protected by barrier landforms, especially rural Alaska communities that rely on coastal resources for subsistence-based livelihood.

### Study Area

Meshik was located on the SE shore of Bristol Bay, near the Aniakchak volcano (Figure 1). The geologic history explains the genesis of surficial deposits and how they influence erosion rates. The settlement history details how Meshik was founded and relocated. This study examines nearly 15 km of shoreline around the townsite.

### Geologic History of Meshik

During the Pleistocene maximum (*ca.* 20,000 YBP), Bristol Bay was above sea level but covered by the Cordilleran ice sheet (Kaufman and Manley, 2004). The ice sheet steadily retreated, and sea levels rose faster than postglacial isostatic rebound, flooding Bristol Bay and even peaking above modern sea level *ca.* 10,000 YBP (Jordan, 2001). The glaciers that carved the Meshik River drainage deposited till and outwash over a vast field of knobs and kettles (Kaufman and Manley, 2004).

The Aniakchak volcano was a glaciated, cone-shaped stratovolcano typical of Aleutian Arc volcanoes. More than 20 postglacial eruptions have been identified since *ca.* 9500 YBP, producing lava flows and depositing ash that formed distinctive

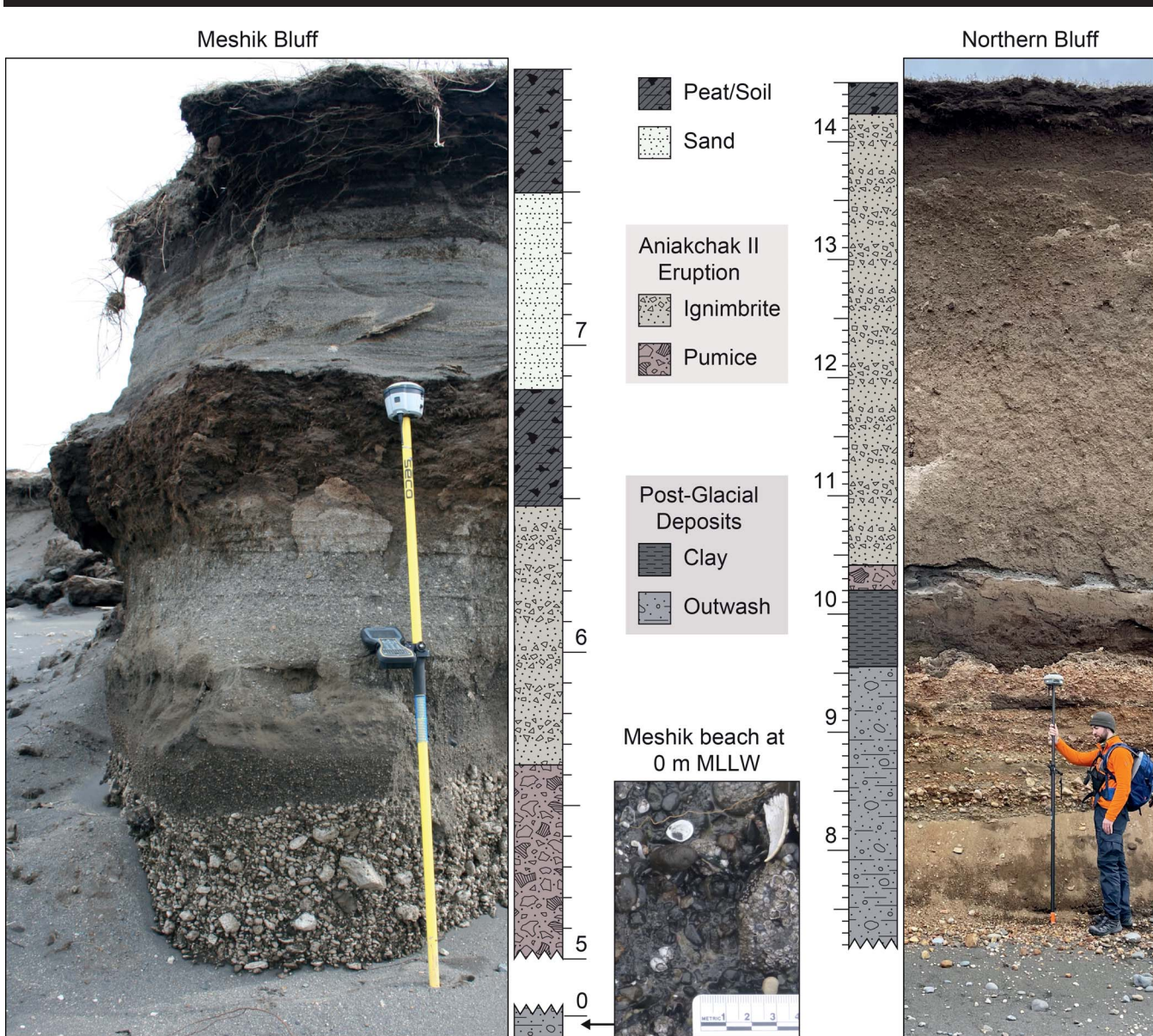


Figure 2. The stratigraphic column of Meshik bluff (left) and northern bluff (right) shows the postglacial, eruption, marine and lacustrine, and soil deposits. The scalebars are in meters above MLLW, and the survey pole is 2 m tall. At Meshik, the exact depth of the Aniakchak II eruption is not known, but the underlying outwash was observed near 0 m MLLW. All layers are nonlithified. Transition heights vary across the shoreline. The postglacial exposure at the northern bluff is typically between 1 and 3 m above the beach. The outwash exposure is partially obscured in the image by collapsed material pressed against the bluff by a storm.

composite layers (Bacon *et al.*, 2014). In  $3660 \pm 70$  cal. YBP, the Aniakchak volcano erupted so violently the entire dome exploded, sending pyroclastic flows into Bristol Bay and blanketing the Alaska Peninsula in ash. This caldera-forming eruption, named Aniakchak II, covered the glacial deposits in several meters of pumice and ignimbrite (pumice-rich ash; Bacon *et al.*, 2014; Figure 2).

Relative sea level had fallen to just above modern elevations around the time of the Aniakchak II eruption, and the Meshik area of the deposit was underwater (Jordan, 2001). A complex interplay of tectonics, glacial isostasy, and eustatic sea-level

change eventually uplifted the submerged landscape. Meshik's volcanic deposits are capped by sand and marine organics, atop which modern tundra soils have formed (Detterman *et al.*, 1981; Figure 2).

To summarize the geologic history, Meshik was built on the tundra soil with layers of unconsolidated volcanic debris below (Figure 2; Detterman *et al.*, 1981). The postglacial deposits under the community are only observable at low tide near the former Meshik coastline. The region is primarily unlithified, nonpermafrost sediments susceptible to erosion by marine energy, especially the pumice, which is less dense than water.

## Settlement History of Meshik

Natural hazards become disasters when people and things of value are endangered. There is an inherent degree of risk when living on the coast, but communities generally find the benefits outweigh the drawbacks. Examining the settlement history helps explore why a community is built at its location and what factors contribute to disasters.

In the 1970s, about 90 people resided in Meshik and relied primarily on subsistence resources, such as fishing, harvesting shellfish and marine mammals, hunting, and berry picking (Lujan *et al.*, 2018). There are no roads to reach this region of Alaska, so most supplies are shipped by barge or brought in by small planes. The community must maintain an isolated grid of infrastructure to provide modern utilities, including generating its own power by burning diesel fuel, treating water for safe drinking, and managing sanitation. These remote and self-reliant characteristics are common throughout most coastal villages in Alaska.

The Sugpiaq (traditional Yupik people indigenous to the Alaska Peninsula) likely began settling the Meshik River area around 1700 cal. YBP (Barton, Shirar, and Jordan, 2018). Migration to the Alaska Peninsula began thousands of years earlier, but geologic changes such as volcanic eruptions and sea-level change either delayed the occupation of the Meshik River drainage or buried evidence (Barton, Shirar, and Jordan, 2018). Because of the Aniakchak II eruption and the time required for terrestrial ecological recovery, the Sugpiaq harvested marine and nearshore resources and lived in semipermanent settlements near the coast (Barton, Shirar, and Jordan, 2018; Morseth, 2003).

The Indigenous society experienced major change with the introduction of outsiders. Beginning in the 1700s, the influx of fur traders, western religion, and fish canneries brought new trade, conflict, culture, and disease (Morseth, 2003). Entire communities were abandoned because of epidemics, economic incentives, and enslavement. By 1867, when the United States purchased Alaska from Russia, Meshik and nearby Unangashak appeared abandoned (Morseth, 2003). The population returned by 1880 and a fish cannery opened, but epidemics in 1900 and 1919 decimated the community and closed the cannery. During a visit in 1931, Hubbard (1952) described Meshik as “a small jumble of barabaras, as the native dugouts are called, with here and there a slightly more pretentious wooden cabin as well as a deserted Russian church and empty cannery building. The village lies on a bar with the sand-choked harbor of Port Heiden on one side and a shallow enclosed lagoon on the other” (p. 50). This description matches the location observed in 1957 imagery, suggesting the shoreline was relatively stable.

Beginning on 3 June 1942 (during World War II), the Japanese Navy invaded the Aleutian Islands. Within just 2 weeks, the U.S. Navy landed on Meshik’s beach and began constructing the Fort Morrow Air Base (Ringsmuth, 2007). This construction included two docks, several miles of gravel road, and two 7500-by-500-foot runways, as well as structures to house and employ nearly 2000 people. The dock pilings were installed in the glacial outwash deposits of gravel and cobbles, and the road and runway gravels were sourced from these

deposits (Community of Port Heiden, *personal communication*; Figure 3).

Many former residents moved back to Meshik to use the amenities and services of the base, namely, the school and health clinic (Ringsmuth, 2007). Most soldiers left after World War II, but the base was used as a White Alice communication site until 1978. These sites provided telecommunications for the U.S. Air Force before satellites, and most of the 40 sites in Alaska were built near remote Indigenous communities. The military removed every structure of the base but left the road system and airport. However, White Alice sites are infamous for polluting the landscape with toxic chemicals, including polychlorinated biphenyl, a substance now banned in the United States. In the mid-1980s, the U.S. Army Corps of Engineers (USACE) and the U.S. Department of Defense began remediating formerly used defense sites, a process that takes decades.

Meshik had been built in the same location since at least the 1800s, indicating a relatively stable shoreline. In the 1970s, storms began rapidly eroding the marine terrace by several meters per year. The community (now called Port Heiden) relocated one home but lost smokehouses to erosion. In 1975, USACE conceptualized a temporary seawall with greatly reduced construction cost by employing Port Heiden residents and using resources from abandoned military structures (Kvasager, 1975). The city enthusiastically prepared to assist in this project and began purchasing construction equipment. However, USACE and state and federal organizations could not justify funding temporary solutions, so no action was taken. Correspondence through 1977 shows that because of miscommunication, Port Heiden still expected state or federal organizations to implement a solution. USACE reported erosion rates averaged 3 m/y in this interim period, and then one storm in November 1978 eroded 30 m and destroyed three houses (Figure 4). In the same year, the Air Force removed all structures from the base, but left a few construction vehicles that the city eventually acquired.

In 1979, Port Heiden began plans to relocate inland along the road system abandoned by the Air Force. There were 26 homes, six city and school buildings, a 1.3-acre landfill of municipal and military waste, two gravesites, and two oil storage towers (Iliaska Environmental Staff, 2008; Legare, 2000). The community had to lead the effort, finding funds for construction equipment, experience, and tools to manage hazardous materials. Most structures were moved in time, but several collapsed onto the beach. Their foundations and buried infrastructure also eroded onto the beach. This included oil barrels, septic tanks, and the landfill (Stergiou, 2013). Port Heiden could not gain funding or assistance to move an influenza mass grave site. Because of a coming storm in 2003, the community spent Thanksgiving Day exhuming and moving ancestors to a safe location (Figure 4). The last structure in Meshik was removed in 2018, and 2 years later the road to the community was undermined by erosion and Goldfish Lake breached into the bay (Figure 4). Relocation took 40 years and a monumental grassroots effort by the community.

The settlement history shows Meshik existed near same location for centuries and erosion only began in the 1970s. With no reason to anticipate rapid erosion, most infrastructure was



Figure 3. (Left) Photograph by Kvasager (1975) showing a structure and car destroyed by a 1975 storm. The beach is composed of glacially derived cobbles in sand. (Right) This picture of the eroded bluff underneath former Meshik shows the cobbles from the beach used for the road system. For scale, the GNSS antenna is 15 cm tall.

built near the coast and became threatened, resulting in a slow-moving disaster that required relocating the entire community.

#### Coastal Setting

The Bristol Bay coastline is segmented by six large embayments that are protected from the open ocean by barrier islands and spits (Sallenger and Hunter, 1984). Port Heiden is situated at the juncture between the inner and the outer parts of Bristol Bay, where the morphology switches from well-developed barrier island systems (typical of wave-dominated coasts) to barrier spits at embayment mouths (typical of tide-dominated coasts; Sallenger and Hunter, 1984). Net alongshore transport is to the NE, but the embayments result in localized sediment transport reversal (Hunter, Sallenger, and Dupre, 1979).

As of 2019, the Port Heiden entrance exhibits the long, narrow Strogonof Point to the south and the wide Chistiakof point to the north. Littoral sediments of Strogonof Point and north of Chistiakof point are well-sorted sands to gravel with abundant pumice float and glacially derived cobbles visible at the surface. Cobbles were last observed on Meshik's beach in 1975, but now the beach is primarily well-sorted sand. Bathymetry charts by the National Oceanic and Atmospheric Administration (NOAA, 2015) show most of the bay is shallow mud flats slightly above mean lower low water (MLLW). The entrance has a series of shoals above MLLW shadowing previous barrier island locations. Shallow channels around

these shoals typically only reach  $-1$  m MLLW. The deepest channel is directly in front of Meshik and reached  $-7$  m MLLW in 1957. With a great diurnal range of 3.54 m (NOAA tide station 9463502), marine vessels safely navigate the bay during high tide.

#### METHODS

The stated objectives are achieved through a combination of field measurements and remote sensing techniques. Authors visited the Meshik townsite in 2013, 2016, 2017, 2018, and 2021 to perform Global Navigation Satellite System (GNSS) surveys and unoccupied aerial system (UAS) surveys and to install community-based erosion monitoring sites. The Native Village of Port Heiden Tribal Environmental Office operated monitoring sites.

#### Historical and Contemporary Shoreline Change

Shoreline change was analyzed by identifying shoreline positions with imagery and GNSS surveys and then measuring the distance between shorelines over time. The bluff top edge (also the vegetation line) was used as the proxy indicator of the shoreline position because it represents the threshold where structures are undermined. Shorelines were delineated in a GIS. Shoreline change was measured using the Digital Shoreline Analysis System tool (Himmelstoss *et al.*, 2018). With user input and validation, this tool draws virtual transects perpendicular to the coastline and computes a change



Figure 4. (A) Residence split in half after a storm eroded the ground underneath. (B) Residents exhume a mass grave site in winter conditions. (C) Fuel barrels and wooden septic tanks eroding from the bluff. (D) Erosion reached Goldfish Lake (left), draining it into Bristol Bay. For scale, see people and the vehicle in the bottom right. Nearly the entire community of Meshik would have been in this camera frame.

rate using the distance and time between shorelines on each transect. The long-term linear change rate was measured using weighted least-squares linear regression (WLR) at a 95% confidence interval.

Shorelines were delineated using satellite and aerial imagery (Table 1). Satellite imagery was georeferenced or orthorectified as appropriate. The 2019 orthoimage was used as the base image to provide control for georeferencing. Scanned frame camera survey photographs were orthorectified using methods by Buzard (2021). Image accuracy was measured to the control image with 20 independent checkpoints. The total uncertainty of shoreline delineation ( $U_t$ ) was computed using the root-sum-of-squares error of three uncertainties, that is, the horizontal fit to the control image (positional uncertainty,  $U_o$ ), the delineator precision ( $U_d$ ), and the image ground sample distance (GSD;  $U_i$ ):

$$U_t = \sqrt{U_o^2 + U_d^2 + U_i^2} \quad (1)$$

To calculate delineator precision, the user delineated a section of coast three times. Precision is the average offset of the delineations. However, delineator precision is affected by factors that improve shoreline interpretation, chiefly pixel size and band resolution. Delineator precision was measured on the lowest-quality image (1973 monochromatic with 1.70 m GSD),

a medium-quality image (1983 color infrared with 1.60 m GSD), and the highest-quality image (2019 color and near-infrared with 0.20 m GSD), achieving 2.37, 2.26, and 1.41 m, respectively. For the remaining imagery, the delineator precision was estimated to be the average of these values (2.01 m).

Shoreline positions at Meshik from 2013, 2016, 2017, 2018, and 2021 were measured using GNSS or UAS surveys. Buzard *et al.* (2021a) orthorectified the 2021 UAS imagery and created a digital surface model, and prior UAS collections were processed using similar methods. Because of the steep bluff, the shoreline was extracted using an elevation contour and then smoothed (for improved comparison to delineated shorelines) and manually corrected using image and field data.

The timing of barrier island reconfiguration was investigated by delineating the waterline in aerial and satellite imagery. To achieve greater temporal coverage, Landsat 1, 2 and 3 images were included. These have GSDs too great for accurate shoreline change detection but still show the barrier islands and their generalized movement. The earliest image was acquired in 1957, so maps before this date were collected. These maps show the general coastal configuration but are not accurate enough for shoreline change measurements.

Table 1. Images used in shoreline change analysis with image GSD ( $U_i$ ), positional uncertainty ( $U_o$ ), delineator precision ( $U_d$ ), and total uncertainty ( $U_t$ ). Collectors are the U.S. Air Force (USAF), Alaska Department of Commerce, Community, and Economic Development (DCCED), U.S. National Aeronautics and Space Administration (NASA), Satellite pour l'Observation de la Terre 5 (SPOT5), Alaska Division of Geological & Geophysical Surveys (DGGS), Worldview 2 (WV2), Quantum Spatial Inc. (Quantum), and one of this study's authors (Buzard). Correction methods include structure from motion (SfM), georeferencing (Georef.), and orthorectifying using ArcticDEM (ArcticDEM).

Shoreline Date	Collector	System	Correction	$U_i$ (m)	$U_o$	$U_d$	$U_t$
1957 June 24	USAF	Plane	SfM	1.24	3.10	2.01	3.90
1963 August 20	USAF	Plane	SfM	0.17	2.78	2.01	3.43
1973 June 22	USAF	Plane	SfM	1.71	3.24	2.37	4.36
1974 July 17	USAF	Plane	SfM	0.33	0.46	2.01	2.09
1983 August 26	NASA	Plane	SfM	1.60	2.50	2.26	3.73
2002 June 17	DCCED	Plane	None	1.00	2.10	2.01	3.07
2009 June 26	SPOT5	Satellite	Georef.	2.50	2.64	2.50	4.41
2013 August	DGGS	GNSS	NA	NA	0.30	NA	0.30
2013 October	DGGS	GNSS	NA	NA	0.30	NA	0.30
2014 May 1	WV2	Satellite	ArcticDEM	2.03	1.81	2.01	3.38
2016 August	Buzard	GNSS	NA	NA	0.30	NA	0.30
2017 May 21	Buzard	UAV	SfM	0.07	0.43	NA	0.45
2018 April 14	Buzard	UAV	SfM	0.05	0.35	NA	0.36
2019 June 27	Quantum	Plane	SfM	0.20	0 (ref)	1.41	1.42
2021 May 7	Buzard	UAV	SfM	0.03	0.08	NA	0.11

NA = not applicable.

### Erosion in High Temporal Resolution

Erosion timing and mechanisms were documented through time-lapse cameras and community-based stake ranging. Two time-lapse cameras were installed near Goldfish Lake to take one picture every hour (Overbeck, Buzard, and Maio, 2017). Staked transects were set up in front of the cameras, parallel to the frame. This approach allows measurements to be made by comparing the distance of the stakes to the bluff edge along their transect. The Tribal Environmental Office measured the distance with a tape measure at least once per year. Measurements from imagery were adjusted to the tape measure and GNSS data to reduce inaccuracy introduced by camera movement.

Alaska's coastal communities experience erosion primarily because of a combination of high tides and waves (USACE, 2009). Storm tide heights are often used to predict or estimate shoreline change (Jones *et al.*, 2018; Leonardi, Ganju, and Fagherazzi, 2015; Vitousek *et al.*, 2017). To describe this relationship, monthly erosion was compared with offshore storm tide heights (tide + significant wave height [SWH]). NOAA provides hourly tidal predictions for Port Heiden. Hersbach *et al.* (2020) published hourly SWH hindcasts. Heights were only used when waves were directed toward Port Heiden.

## RESULTS

Results are divided into two sections to discuss erosion of the barrier islands and the mainland. The focus of these results is to determine the erosion timeline and identify main drivers and mechanisms.

### Barrier Island Reconfiguration Timeline

The reconfiguration of Chistiakof Island was a pivotal event. Maps from France, Russia, and the United States roughly show an island existed as early as 1828 and was located near the center of the bay mouth (Figure 5). By 1924, the elongated barrier island chain crossed the bay and Strogonof Point formed into a long spit. These early maps are not reliable for accurate island shape and position but confirm barrier islands

persisted in Port Heiden since at least the early 1800s. Written accounts collected by Morseth (2003) suggested the Meshik

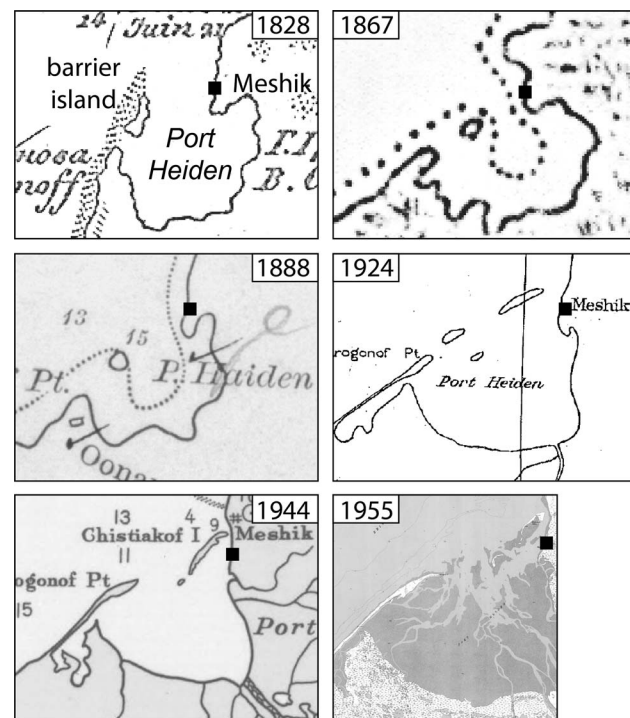


Figure 5. Maps illustrating Port Heiden from 1828 to 1955. Maps are not to scale and are not anticipated to accurately depict the shoreline in fine detail, especially further back in time. Meshik (black square) was first labeled on a map in 1924, so the position is estimated from 1828 to 1888. This comparison shows a general trend from a southwestward slightly elongated island to a northeastward elongated island, as well as the growth of Strogonof Point. Maps are by Khoudchine (1828), Lewis (1867), the U.S. Commission of Fish and Fisheries (1888), Smith and Baker (1924), the U.S. Coast and Geodetic Survey (1944), and the U.S. Geological Survey (1963; Port Heiden area based on 1955 data).

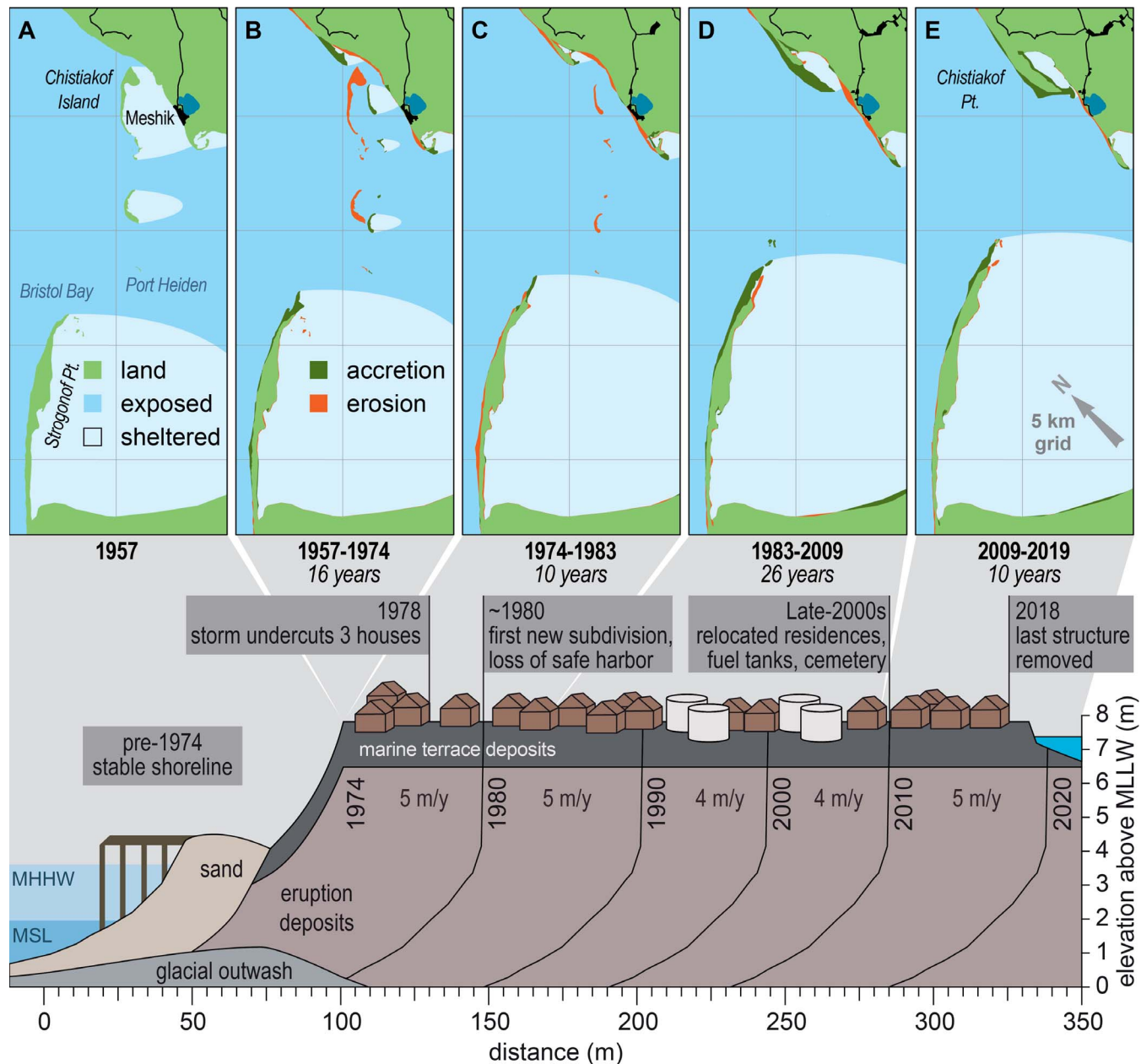


Figure 6. Erosion history of Meshik. (A–E) Timeline of barrier island and coastal erosion (orange) and barrier migration and formation (dark green). Coarse estimates of sheltered (light blue) and exposed (blue) waters conceptualize how the barrier reconfiguration influenced waves reaching Meshik. The lower plot shows the stable shoreline from 1957 and the erosion timeline, normalized by decade with inferred beach elevation profiles based on 2021 profile 102 at the former townsite. From 1957 to 1974, the barrier islands shrank and migrated toward the coast. Erosion began north and south of Meshik. After 1974, the islands submerged and erosion at Meshik increased to 5 m/y on average.

shoreline was stable during this period. There was traditional infrastructure from the original village, as well as a saltery operated by the Port Heiden Packing Company. The bay was deeper (Morseth, 2003), and the protective barrier islands provided a safe harbor for ships (Ringsmuth, 2007). The existence of barrier islands and community infrastructure for more than a century shows that the rapid erosion was unprecedented.

Figure 6 shows the history of barrier island migration (measured through aerial imagery) and community relocation. In 1957, 5.3 km of barrier islands crossed the entrance of Port Heiden, leaving three main openings of 5.0, 1.2, and 0.5 km in width. Between 1957 and 1973, the islands shrank and migrated toward the coast. Rapid coastal erosion occurred north and south of Meshik. The island is last seen in an aerial photograph acquired in summer 1977 by USACE. It completely

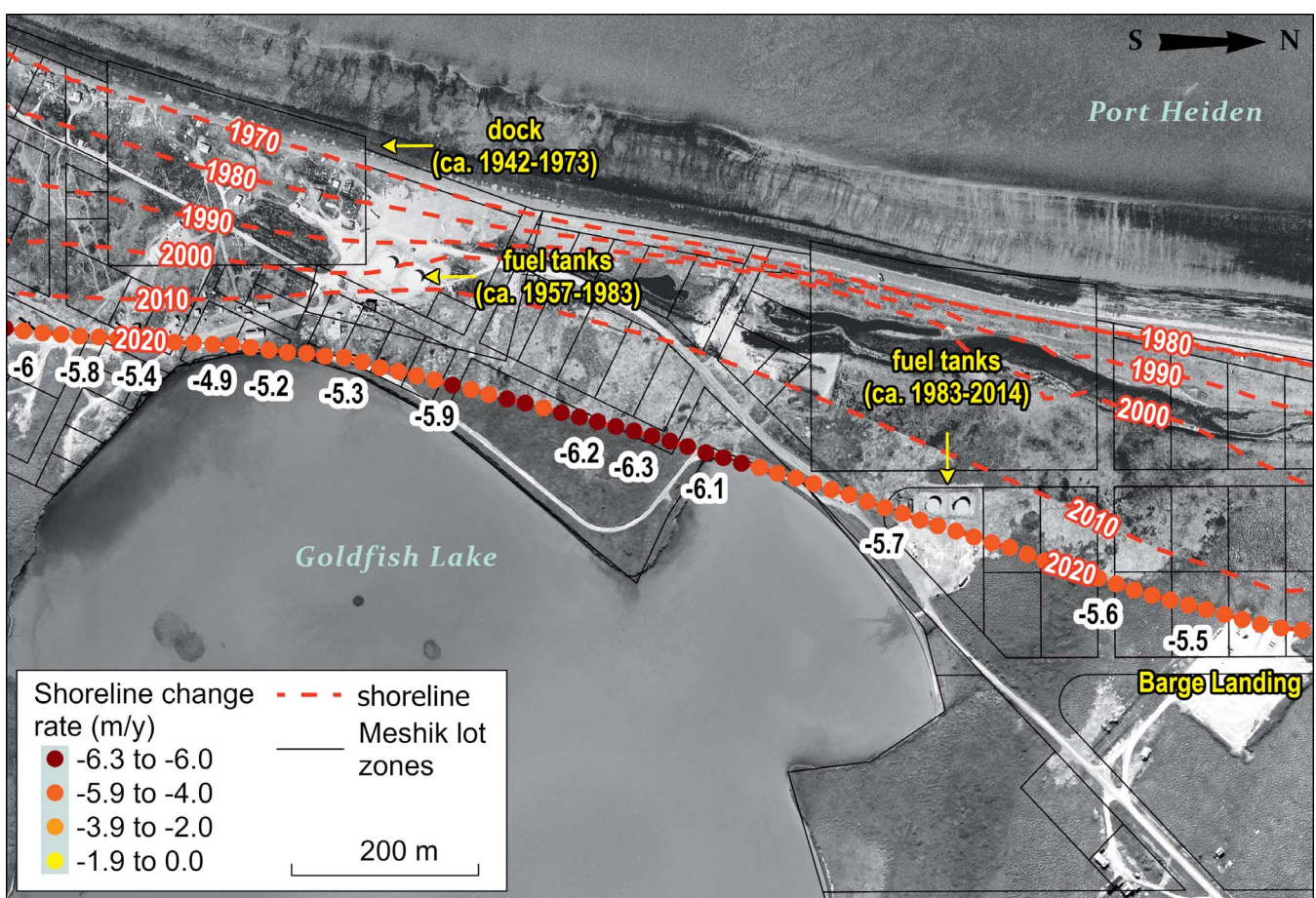


Figure 7. Shoreline positions interpolated per decade (dashed red lines) show the erosion history of Meshik. Most structures were built at the south end of the lake, but the zoned lots show how much property Meshik lost to erosion. The image is a composite from different periods to showcase infrastructure. The image of the shoreline is from 1974, showing the village, original fuel tank location, and the spit and back-barrier lagoon extending to the east. Barges landed near the dock, which had recently been destroyed by sea ice. At the 2010 line, the image is switched to 2002 to show the remaining structures to be relocated and the location to which the fuel tanks were moved. At the 2020 line, the image switches to 2019 to show the new barge landing site. The 2020 shoreline is symbolized by the WLR shoreline change rates from 1974 to 2021.

eroded by July 1978 (observed in Landsat imagery). That November, a storm eroded 30 m of coastline and destroyed three homes, prompting the urgent relocation effort. Erosion rates sustained 4 to 5 m/y on average, punctuated by storms. Chistiakof point formed by 1974 and extended nearly 2 km by 2009. Strogonof Point also extended by 3 km from 1957 to 2019. Although these two spits grew several kilometers into the bay, the Meshik coastline remained exposed. Nearly the entire community footprint eroded by 2019.

#### Shoreline Change

The Meshik shoreline was stable from 1957 to around 1973. From 1974 to 2021 (47 years), erosion rates increased to 5.8 m/y (standard deviation [SD]=0.3 m/y), on average, eroding around 270 m inland (Figure 7). Erosion rates were linear at the southern section of the town site, where most structures were located. The elevation profiles from 2013 to 2021 (Figure 8) showed beach erosion followed bluff erosion but the volume of sand increased, resulting in a wider and less steep beach. This

resulted from an outwash sand lobe that formed from the breach of Goldfish Lake. The northern section was fronted by a sand spit and back-barrier lagoon. These features took 30 years to erode. After being exposed, the remaining bluffs eroded about 200 m in 10 years, catching up to the total erosion distance of neighboring shorelines.

The bluffs north of Chistiakof point have a stratigraphy similar to that of Meshik and were never protected by barrier islands during the study period. From 1957 to 2019 (62 years), these bluffs eroded between 190 and 320 m, averaging 3.3 m/y (SD = 0.5 m/y; Figure 9). Approximately half of this erosion occurred over the first 17 years, with rates as fast as 10.5 m/y. After 1974, erosion rates slowed to between 1.9 and 3.4 m/y. Two elevation profiles were collected near where Chistiakof point begins. From August 2013 to April 2018 (5 years), the bluff did not erode but the mean higher high water line eroded 27 m, resulting in a steeper beach (Figure 10). Grain size increased from some cobbles in a sandy matrix to a cobble berm. This could represent the temporary change in beach morphol-

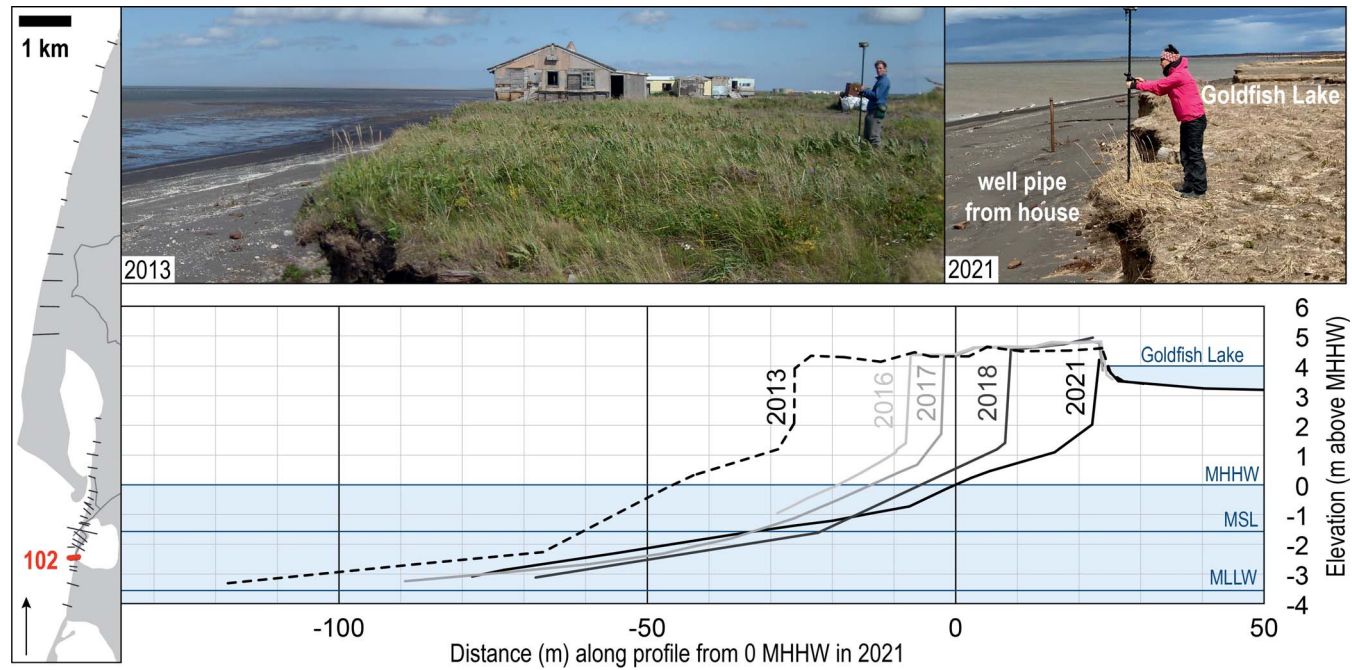


Figure 8. Elevation profiles at the Meshik townsit show steady erosion of about 50 m over 8 years (6 m/y). The beach elevation rose between 2018 and 2021, coinciding with when Goldfish Lake breached. All structures in the top image were removed by the City of Port Heiden.

ogy caused by seasonal shifts in marine energy, or it may result from a recent storm. The largest storm over the study period occurred in February 2018, 2 months before the latter profile. These observations show exposed areas of Port Heiden experienced high marine energy and regular erosion throughout the study period, supporting the assumption that the barrier islands protected Meshik's shoreline.

The formation of Chistiakof point altered the erosion rates of the coastline behind it. In 1957, a series of sand spits existed

between Meshik and northern bluffs, deposited by longshore currents. By 2002, the spits had disappeared, and the shoreline eroded 200 m (Figure 9). Over this period, deposited sediments formed a 2-km spit (accreting 44 m/y on average). This also protected the back-barrier coastline, and it began to stabilize. The spit reached more than 3 km by 2019, with the point nearly touching the mainland at the barge landing. Elevation profiles in the back-barrier showed a switch from erosion to accretion that followed the spit formation south (Figure 11).

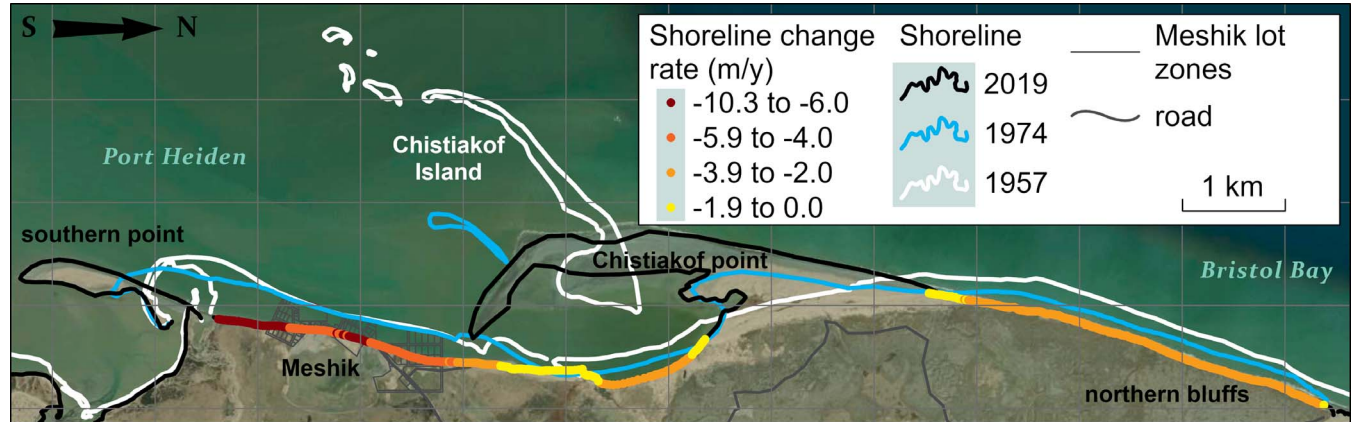


Figure 9. Shoreline change map of Port Heiden from Meshik to the northern bluffs. Shoreline change rates are symbolized with hot colors along the 2019 shoreline. Negative values indicate erosion. The black sections of the 2019 shoreline accreted or were not measured. The 1957 (white) and 1974 (blue) shorelines show the erosion timing and extent, as well as the reconfiguration of Chistiakof Island into a spit. Shorelines represent bluff top edges or vegetation lines. The shorelines of the islands and spits represent high-water lines. Most of Meshik's zoned lots (gray) eroded by 2019 (Image: Earthstar Geographics, ca. 2021).

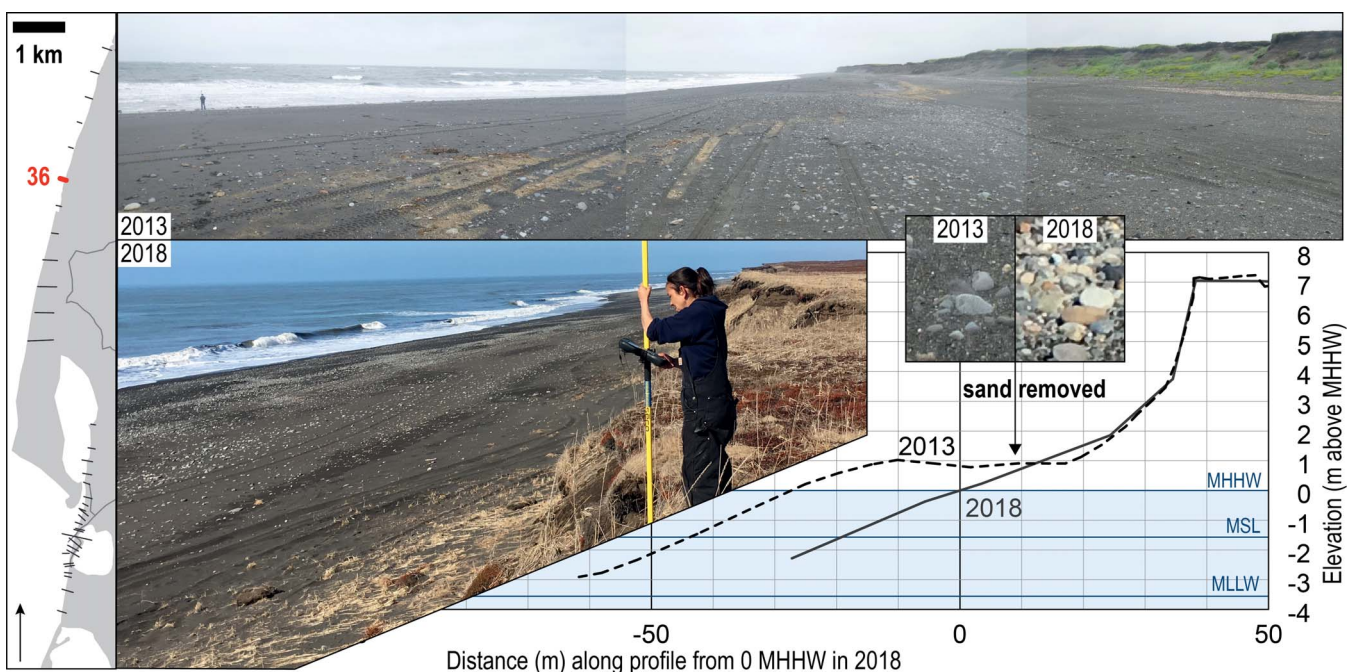


Figure 10. Elevation profiles north of Chistiakof point between August 2013 and April 2018 show bluff stability but beach erosion. The broad, sandy berm eroded away, leaving a ridge of glacially derived cobbles. This is likely the result of the February 2018 storm.

### Erosion Drivers and Mechanisms

Erosion measurements from time-lapse imagery, community-based stake ranging, and GNSS show a high-resolution record from August 2016 to May 2021 (Figure 12). Erosion rates averaged 6.6 and 7.9 m/y at the south and north ends of Goldfish Lake, respectively. Erosion can occur year-round but was greatest from November into January, the fall to winter season, when water levels and storm activity were high (Figure 13). The February 2018 storm was an outlier in both timing and intensity. This event eroded 6 to 10 m of bluff, exceeding average annual erosion overnight.

The greatest erosion occurred during the greatest storm tide, but storm tide is not a reliable predictor of erosion (Figure 13). This may be explained the cyclical bluff erosion mechanism of undercutting and collapse. Although the bluffs comprise nonlithified sediments, they can support vertical faces and overhangs. After sufficient erosion of the pumice and sand, the overhanging peat layer separates and collapses onto the beach (Figure 14). It can require multiple small storms to undercut enough for a collapse, resulting in bluff top erosion rates lagging the heightened storm tide in October.

### DISCUSSION

The erosion history of Meshik shows unprecedented, rapid, and unrelenting changes unfolding over short timescales, posing significant challenges for a remote polar community. Erosion is primarily caused by storms and waves during high tide. Meshik had the fourth-fastest erosion rate of Alaska communities (Overbeck *et al.*, 2020). This speed partially resulted from the poorly welded volcanic layers of pumice and

sand that erode rapidly during storms. The northern bluffs have a stratigraphy similar to that of Meshik but at higher elevation, revealing the preeruption glacial deposits at the beach surface (Figure 2). These range from clay to cobbles and are more resistant to erosion than pumice and sand, resulting in slower erosion rates than in Meshik (Figure 9).

The shift from a stable to an eroding coastline is attributed to the loss of protective barrier islands, increasing the wave energy reaching Meshik. This conclusion is supported by observing the erosion of the northern bluffs that were exposed while Meshik was sheltered (Figure 9). The discussion covers possible reasons the barrier islands eroded and the broader impacts and implications for coastal communities.

### Erosion and Infrastructure Planning

Although Port Heiden relocated all structures out of the eroding area, the community still relies on the Meshik coastline for marine resources, especially commercial and subsistence fishing (Lujan *et al.*, 2018). The loss of a safe harbor to store and launch boats is a particularly acute challenge. Residents and city planners have explored the possibility of using the Goldfish Lake area to construct a harbor. The highly erodible pumice and ignimbrite continue underneath Goldfish Lake, where there is no further peat layer. These sediments make the drained lake basin unsuitable for long-term infrastructure development.

Chistiakof point ends at the barge landing. If the spit continues to migrate south, it could provide protection to the coastline. However, the intense curl that formed around 2009 may indicate an end point to alongshore growth. If this is the case, the spit could continue to direct waves and longshore

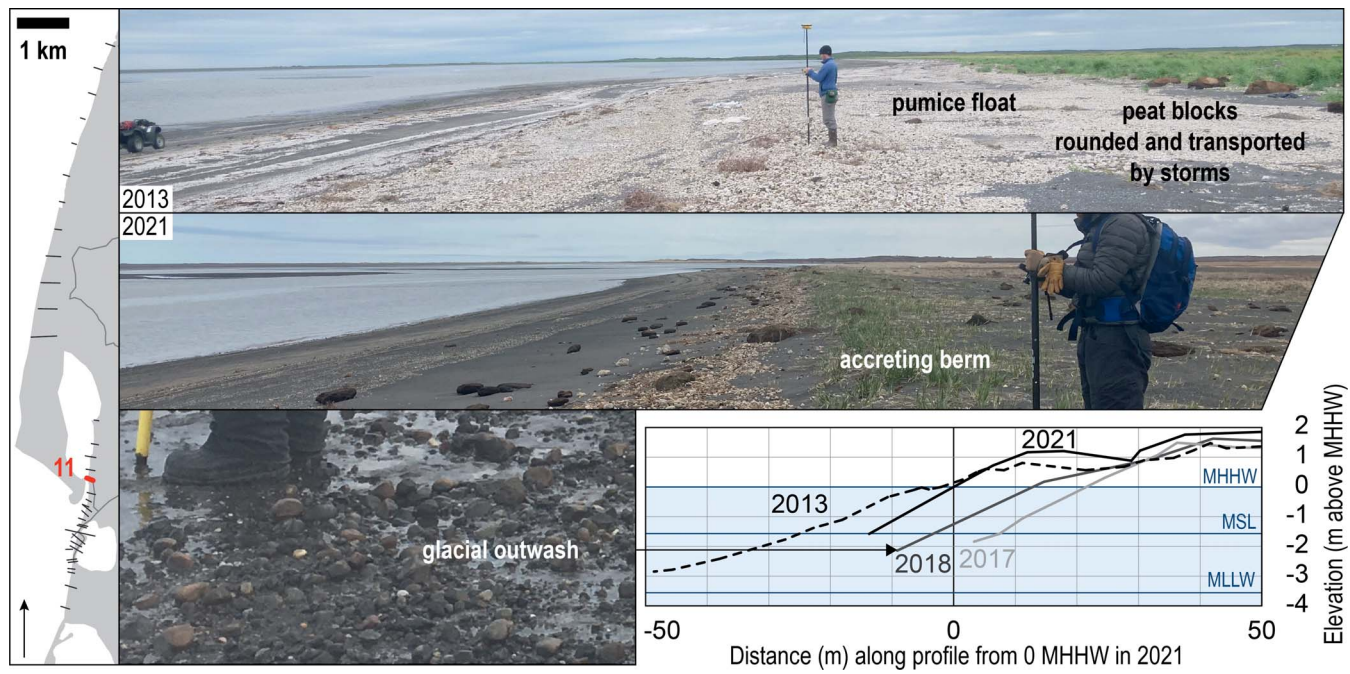


Figure 11. Elevation profile 11 behind Chistiakof point shows beach erosion from 2013 (dashed) to 2017 (light gray) and then accretion. The switch to accretion occurred earlier for back-barrier profiles farther north. Residents observed this area flooding during large storms, evidenced by the floated pumice, blocks of rounded peat, and small cobbles.

currents to the barge landing and erode the Meshik coastline. The back-barrier accretionary coastline is a low-elevation drained lakebed that still floods during large storms. The community constructed a gravel road to launch boats safely in this area, but the active floodplain prevents the safe construction of permanent infrastructure. Ultimately, this coastline is still undergoing large, dynamic changes that will continue to challenge coastal infrastructure planning (Buzard *et al.*, 2021c).

#### Barrier Island Reconfiguration and Oceanographic and Meteorological Change

Barrier islands and spits are transient features formed by the dynamic interplay of sediment deposition and transport (Davis, 1994). Island shape was believed to be tightly coupled to the ratio and magnitude of marine and wave energy (Davis and Hayes, 1984; Hayes, 1979). However, Mulhern, Johnson, and Martin (2017) found more than 90% of island shape is explained by other factors, including tectonics, climate, vegetation, ice, storms, underlying substrate, preexisting topography, shelf slope and width, relative sea-level change, headland and embayment geometry, proximal subenvironments, longshore currents, tidal prism, and anthropogenic alterations. Although a separate analysis is required to fully understand the cause of Chistiakof Island's reconfiguration, there are key factors that likely contributed.

#### Tidal Range

Many factors influence the perseverance of barriers, but islands tend to only persist where the tidal range is below 3.5 m and mean annual SWH is below 3 m (Mulhern, Johnson, and

Martin, 2017). Port Heiden's tidal range was 2.59 m in 1957 (Table 2), exceeding the tidal range of 96% of the barrier islands observed by Mulhern, Johnson, and Martin (2017). Large embayments have transitioned from wave- to tidal-dominated coastlines, and the estimated tidal range limit occurs near Egegik (Figure 15). Maps as early as 1828 and continuous aerial imagery of the Alaska Peninsula in the 1950s support this estimate, showing the Chistiakof Island chain was one of only two islands in the four embayments between Port Heiden and Naknek (Sallenger and Hunter, 1984). The other island, about one-quarter of the size of Chistiakof, still exists as a 1.3-km-long sandbar at the mouth of the Egegik River (tidal range of 3.7 m). Chistiakof Island's position near the tidal limit likely made it more reliant and susceptible to other factors that control island morphology.

#### Sea-Level Rise

Simulations by Nienhuis and Lorenzo-Trueba (2019) estimated barrier islands can be drowned by relative sea-level rise (RSLR) as low as 3.5 mm/y, but rates of 4 to 8 mm/y or greater are more likely required. Natural gravel barriers with a high cross-sectional area, like those in Port Heiden, can withstand greater sea-level rise rates if sediment is not removed from the system (Pollard *et al.*, 2022). The two tidal datums computed for Port Heiden show mean sea-level rates were  $0.00 \pm 1.00$  mm/y between 1957 and 2013 (Table 2; datum computational error of 0.0396 m from NOAA, 2003). DeGrandpre and Freymueller (2019) estimated the vertical land motion is  $-1.00 \pm 0.35$  mm/y, resulting in RSLR of  $1.00 \pm 1.06$  mm/y. The limited datasets for this calculation warrant a comparison

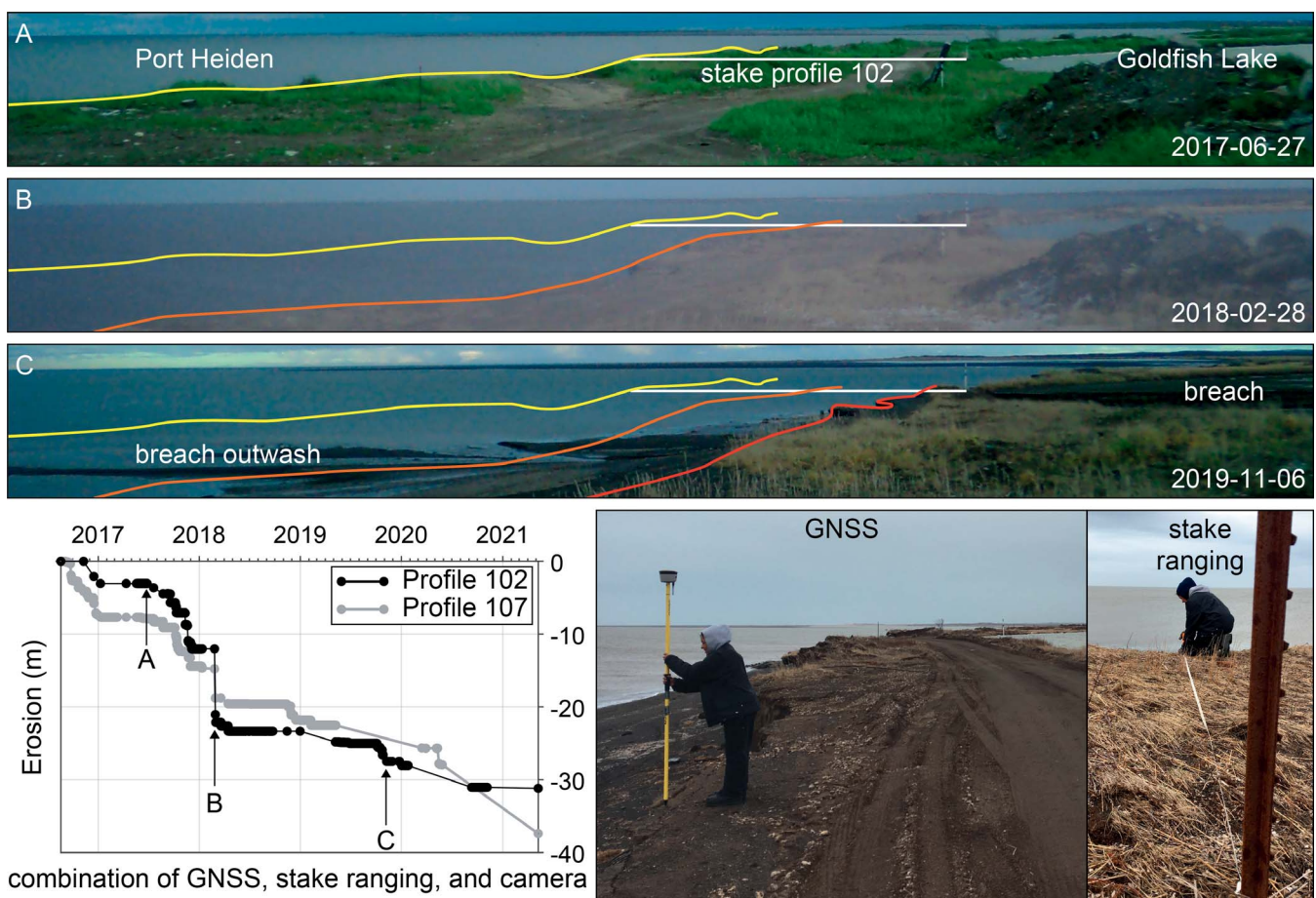


Figure 12. Erosion measurements at the former townsite of Meshik. (A–C) Time-lapse photos with annotated shoreline positions (sequentially yellow, orange, and red) and stake profile 102 (white) used for the plot below. The plot shows erosion along two profiles at either end of Goldfish Lake. Erosion typically occurred gradually, although one storm caused 6 to 10 m of erosion (B) on 28 February 2018. The bottom-right photos show Port Heiden Tribal Environmental Office staff measuring the bluff edge with GNSS and with measuring tape from a stake.

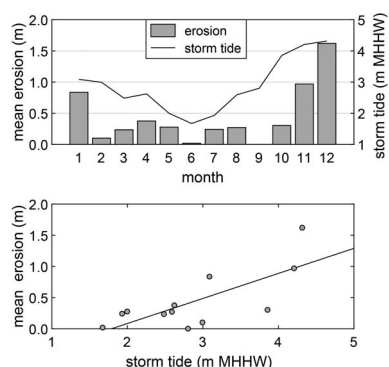


Figure 13. (Top) Mean monthly erosion distance (bars) compared with the average maximum offshore storm tide (tide + SWH). October through February have the greatest storm tide, but erosion is greatest from November through January. (Bottom) Linear regression shows that the maximum monthly storm tide somewhat explains erosion but is not statistically significant ( $y = 0.402x - 0.719$ ,  $R^2 = 0.54$ ,  $p = 0.07$ ).

to a more reliable station. Port Moller (150 km SW) provides the nearest RSLR calculation from long-term tidal measurements, showing  $3.31 \pm 1.79$  mm/y from 1984 to 2021 (missing data from 1990 to 2005; NOAA Center for Operational Oceanographic Products and Services station 9463502). Neither result has adequate inputs for a confident RSLR rate and would be likely to cause island submergence on its own (Nienhuis and Lorenzo-Trueba, 2019).

#### Wave Energy and Storms

SWH is used to quantify the influence of waves (Hayes, 1979). Port Heiden's mean annual SWH is 1.14 m (Figure 16; Hersbach *et al.*, 2020), a common value for barrier islands (Mulhern, Johnson, and Martin, 2017). Storm surge and high water for long durations lead to the greatest erosion at Meshik (Fathauer, 1978; Kvasager, 1975), so SWH greater than the 97.5th percentile of waves is examined (Figure 16). There is no major difference in extreme SWH in the 1960s to 1970s compared with the study period, but 1959–74 was consistently stormy. Typically, there is greater interannual variability,

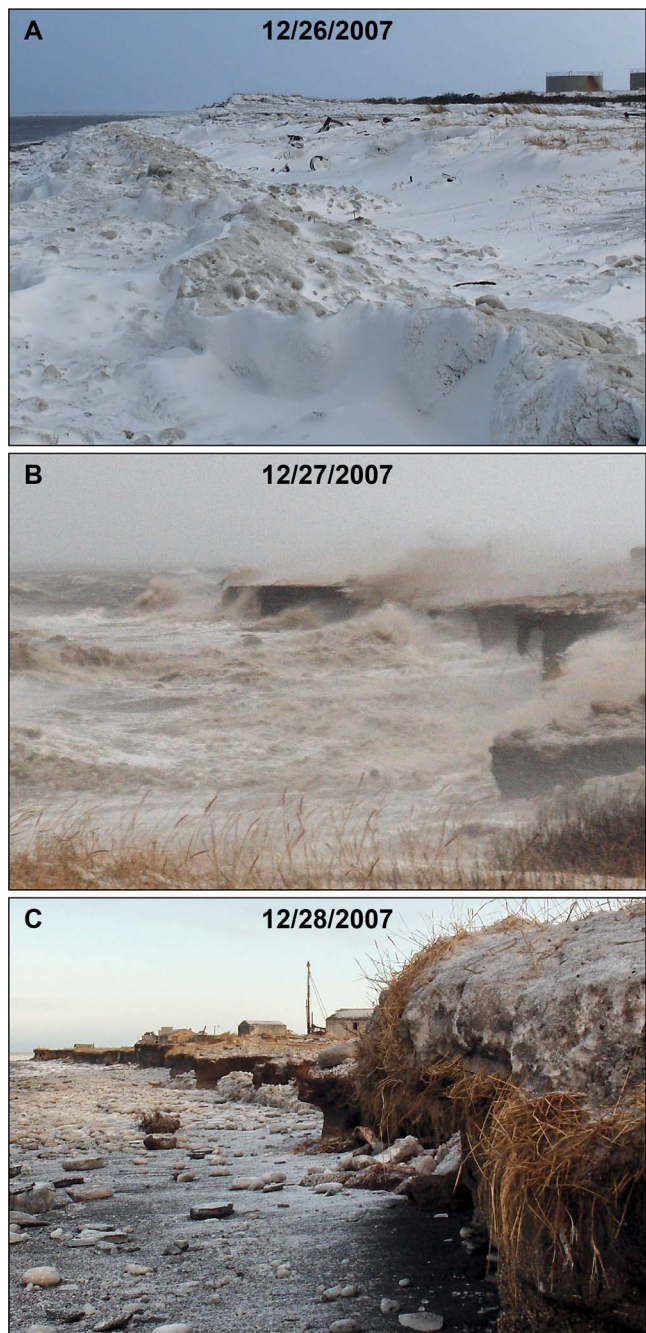


Figure 14. Three photos of the December 2007 storm showcase a typical storm eroding the bluff at Meshik. (A) The beach is covered in about half a meter of snow before the storm. (B) The storm tide reaches the bluff toe, and waves crash into the face. Bluffs have a vertical angle. (C) After the storm, the bluff is undercut and layers of peat are overhanging and slumping. The beach is covered in rounded ice and peat blocks.

expressed by the SD (Figure 16). Coastal features achieve equilibrium by recovering after disturbances like storms. The continuous storminess in this period may have pressured Chistiakof Island toward an erosional regime.

A key question is whether storm activity during the hindcast period deviated from prior conditions. Over the 20th century, there was no significant change in the frequency or intensity of storms entering the Bering Sea, but there were decadal variations in track and strength (Mason, Salmon, and Ludwig, 1996; Mesquita, Atkinson, and Hodges, 2010; Rodionov, Bond, and Overland, 2007; Terenzi, Jorgenson, and Ely, 2014). From the late 1950s to 1976, there was an increase in Bering Sea storms tracking east into Bristol Bay (Mesquita, Atkinson, and Hodges, 2010; Pease, Schoenberg, and Overland, 1982). Average storm intensity increased over this period, especially in the 1960s, and had greater frequency in the 1970s (Mesquita, Atkinson, and Hodges, 2010). This storm climate correlates with a high North Pacific index occurring from 1947 to 1976 (Rodionov, Bond, and Overland, 2007). A high index also occurred from 1901 to 1924 and again correlates with greater storm activity (Mason, Salmon, and Ludwig, 1996; Rodionov, Bond, and Overland, 2007; Terenzi, Jorgenson, and Ely, 2014). Altogether, these studies illustrate a period of heightened storm activity while Chistiakof Island eroded, although this level of activity is common on a centennial scale.

Port Heiden also experiences storms that travel into Bristol Bay from the Gulf of Alaska. These move over the Alaska Peninsula, diminishing storm surge generation. Alaskan track storms have greater intensity and frequency than Siberian track storms (Rodionov, Bond, and Overland, 2007). Although there is less potential to generate surge in Bristol Bay, extreme winds increase wave action and cause coastal damage. For example, in March 1957, an Alaskan track storm destroyed one of Port Heiden's docks through a combination of wind, waves, high tide, and sea ice (U.S. Weather Bureau, 1957). Alaskan track storm frequency and intensity have increased over time because of global warming, with a marked shift in 1976–77 as the Pacific Decadal Oscillation switched (Bromirski *et al.*, 2013; Hartmann and Wendler, 2005; Mantua and Hare, 2002; McCabe, Clark, and Serreze, 2001; Wang, Kim, and Chang, 2017). However, from 1940 to 1977, there were fewer Alaskan track storms than usual entering Bristol Bay (Rodionov, Bond, and Overland, 2007).

#### Sea Ice

In polar regions, sea ice can be a proxy for wave energy; sea ice can diminish wave energy, and conversely sea ice reduction increases wave energy (Overeem *et al.*, 2011; Vermaire *et al.*, 2013). Sea ice reduction can allow barrier systems to reconfigure more rapidly (Farquharson *et al.*, 2018). The sea ice margin demarcates a threshold at which waves are damped by sea ice cover and is defined as ice concentrations reaching or exceeding 15% (Overeem *et al.*, 2011). Sea ice concentration data are available from 1850 onward (Walsh *et al.*, 2017). From 1850 to 1976, there were typically between 100 to 150 ice d/y offshore of Port Heiden (Figure 17). Beginning in the 1950s, ice days became more variable year to year and followed a general decline. After 1976, sea ice declined rapidly. Walsh and Johnson (1979) observed this general decline in Bering Sea ice, with notable lows in the 1960s.

Table 2. Port Heiden tidal datums measured in 1957 and 2013 relative to mean sea level, controlled by benchmark Meshik 1949 (PID UW1437). The benchmark matched its installation description, suggesting it was not disturbed. The elevation of the benchmark above mean sea level did not change.

Datum	Elevation in 1957 (m)	Elevation in 2013 (m)	Change (m)
Benchmark	6.1	6.1	0.00
Mean higher high water	1.66	1.59	-0.07
Mean high water	1.29	1.24	-0.05
Mean sea level	0.00	0.00	0.00
Mean low water	-1.30	-1.24	+0.06
Mean lower low water	-2.09	-1.95	+0.14
Mean tidal range	2.59	2.48	-0.11
Great diurnal range	3.75	3.54	-0.21

### Summary of Chistiakof Island Reconfiguration

#### Drivers

The discussed environmental variables illustrate a combination of factors influencing island reconfiguration. Chistiakof Island existed since at least the early 1800s, possibly becoming more elongated and moving NE as Strogonof Point formed (Figure 5). It is uncommon for barrier islands and spits to prevail in the high tidal range, but erosional and depositional processes were evidently in equilibrium. From the 1950s to 1973, the island was greatly reduced, and it completely eroded around 1977. Strong storms more frequently entered Bristol

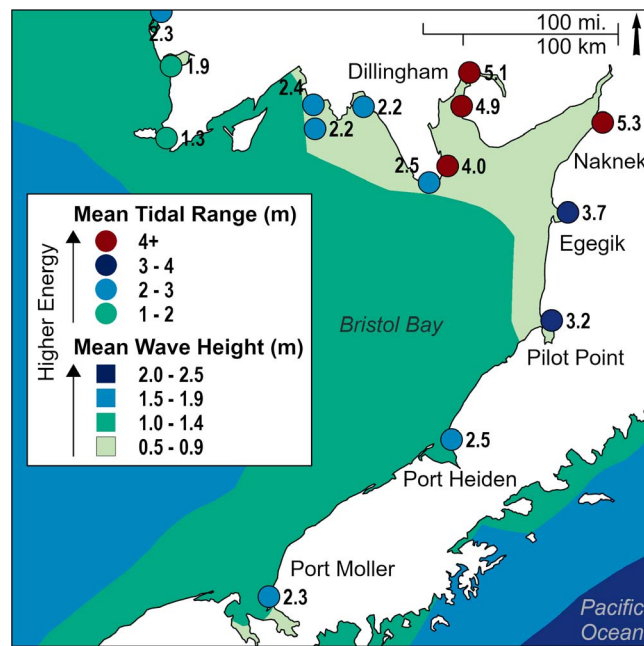


Figure 15. Mean tidal range (circles) and mean wave height of Bristol Bay. Green to blue symbolizes low to high energy conditions (respectively) where barrier islands could exist. Tidal ranges exceeding the limit of barrier islands are in red. Wave heights decrease and tidal range increases toward the head of the bay (NE). Tidal datums were provided by the NOAA Center for Operational Oceanographic Products and Services in 2021. Wave heights were calculated from monthly average SWH hindcasts by Hersbach *et al.* (2020).

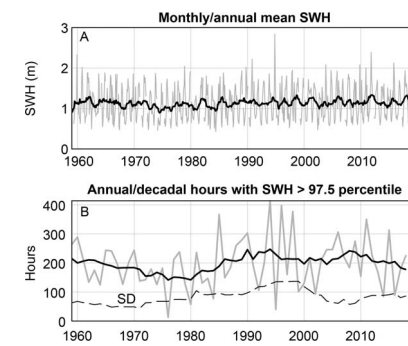


Figure 16. (A) Monthly (gray) and annual (black) SWH at Port Heiden. (B) Annual (gray) and decadal (solid black) hours when SWH is greater than the 97.5th percentile of the dataset. The decadal SD (black dashed) shows interannual variability. SWH is controlled for wave directions toward Port Heiden. SWH is not calculated when sea ice is present.

Bay over this period, allowing less time for the barrier islands to recover (Figure 16). The increased storminess was not unusual, but sea ice also went into decline and became more variable. This increased net wave energy and the likelihood of storms making landfall. Even though the 1970s saw brief sea ice recovery, the island was already greatly reduced, and the community observed continuous storms erode the island remnants (Kvasager, 1975). After this point, sea ice declined significantly, and the island never reformed.

The island's erosion appears to be attributed to a combination of increased storms and decreased sea ice in an area with a high tidal range already stressing barrier islands. However, there are many significant controls of barrier islands that must be examined, including changes to the sediment budget, currents, nearshore ice, and possible anthropogenic activity (Mulhern, Johnson, and Martin, 2017; Reimnitz, 1990).

#### Broader Impacts and Implications

Several Alaska communities have considered relocating because of coastal hazards (U.S. Government Accountability Office Staff, 2022). Fortunately, few experience erosion rates like Meshik; among Alaska communities with computed erosion rates, Napakiak and Newtok are the only locations to exceed Meshik's erosion rates near infrastructure (sustaining 12.8 and 22.2 m/y since the 1950s, respectively; Overbeck *et al.*, 2020). Like Meshik, Napakiak has gradually relocated struc-

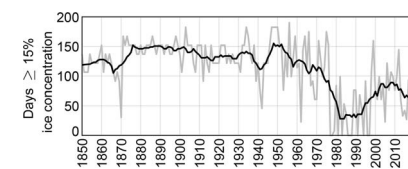


Figure 17. Days per year when sea ice concentration is sufficient to dampen wave energy. The gray line is the annual number of days, and black is the 10-year average. Days averaged between 100 to 150 d/y from 1850 to 1976 and then plummet to less than 100 d/y. Measurements were taken approximately 25 km offshore of Port Heiden.

tures inland since at least the 1950s—although with great losses, including the erosion of a new K–12 school in the 1970s and the replacement school around 2022. Newtok is built in a thawing permafrost delta and did not have suitable land to move structures, so the community is relocating to a nearby rocky island with a stable shoreline. Many other communities with slower erosion rates have successfully implemented rock revetments or seawalls to mitigate erosion and delay or even prevent relocation (Buzard *et al.*, 2021c).

A limitation to erosion predictions is the assumption that boundary conditions will stay the same, resulting in future erosion continuing past patterns. This study demonstrates how barrier island reconfiguration can bring unprecedented erosion to a historically stable shoreline. Sea ice influences sediment transport (Reimnitz, 1990), and Farquharson *et al.* (2018) identified a link between sea ice decline and increased barrier island reconfiguration. Major sea ice decline has already been observed in the Arctic, and models suggest greater decline is ahead (Yadav, Kumar, and Mohan, 2020). Many polar communities are protected by barrier islands and spits, and several are built on these features. As warming and sea ice decline continue, these communities will have a greater likelihood of erosion regime change.

Meshik's rapid erosion rates were partially attributed to easily erodible soils. Most coastal communities in western and northern Alaska are located on unconsolidated gravel, sand, or mudflat shorelines, which are more susceptible to erosion than rock substrates (Overbeck *et al.*, 2020; ShoreZone, 2022). Sediments are a major factor for the two communities with faster erosion, Napakiak and Newtok. Like Meshik, Napakiak's coastline has unlithified, well-sorted sand with no permafrost, allowing rapid erosion at the bend of the Kuskokwim River estuary (Buzard *et al.*, 2021c). Newtok is built on unlithified deltaic soils with thawed permafrost that are easily eroded during floods in a process of land collapse called *usteq* in Yupik (Bronen *et al.*, 2020). Permafrost coastlines are susceptible to degradation and erosion, particularly when thawed by increased warming (Irrgang *et al.*, 2022). Sandy barriers are also more susceptible to reconfiguration as sea ice declines (Farquharson *et al.*, 2018).

A unique observation from this study is the natural process causing the shift from a safe to a hazardous coastline, rather than an anthropogenic source. Many Alaska communities have relocated because of erosion and/or flooding, including Mertarvik (formerly Newtok), Shaktoolik, Napakiak, Point Lay, Alakanuk, Goodnews Bay, and Nunam Iqua (formerly Sheldon Point). These were built in previously unidentified hazard-prone areas, so relocation was inevitable. In contrast, Meshik was built in a safe location until the barrier island eroded. If climate change leads to increased reconfiguration of barrier islands and spits, Alaska would see more erosion concerns from communities with historically stable shorelines, especially those on susceptible soils.

Meshik's experience highlights financial, social, and cultural stresses that accompany a successful relocation. Relocation is generally a last resort and introduces new challenges. Buzard *et al.* (2021c) and Bronen and Chapin (2013) discussed cases in which communities were cut off from funds to maintain essential infrastructure after just voting to relocate or were

the subjects of disastrously overpredicted erosion rates. Port Heiden sought protection in place but could not meet the cost-benefit ratio required for a federally constructed seawall. The community had to manage its own relocation, which is a monumental task for small, rural, subsistence-based villages in Alaska. Because of expansive wetlands, the community had to relocate more than 2 km inland. Toxic soil from previous military activity caused concern for clean water resources and took decades to remediate. The distance of relocation requires residents to own and maintain vehicles to participate in coastal subsistence activities. There is no longer a safe harbor, so boats must launch and land in dangerous open ocean conditions (Lujan *et al.*, 2018). As more communities debate erosion responses, careful consideration must be made to identify the broader impacts of these decisions.

## CONCLUSIONS

A thorough examination of shoreline change was conducted using historical maps, remote sensing data, and field surveys to identify the causes and mechanisms of erosion that threatened the Alaska Native village of Meshik. A barrier island had protected the community since at least the early 1800s but quickly eroded away in the 1970s. This allowed wave and storm energy to reach and erode unconsolidated sediments underlying Meshik. The nonlithified pumice underneath the village was easily eroded by an elevated marine energy regime. Between 1973 and 2021, erosion rates were  $5.8 \pm 0.6$  m/y on average. Storms had the potential to erode 10 to 30 m. Erosion destroyed homes and forced the community to relocate, abandoning the coastal townsite to establish a new city inland. Erosion of the safe boat harbor and relocating inland disrupted the traditional way of life. Although erosion is common in Alaska coastal communities, it is rare for a stable shoreline to suddenly and rapidly erode. Nearly two decades of heightened storm activity and declining sea ice contributed to the erosion of the protective barrier island. Attempts to connect environmental conditions to erosion rates are limited by the availability of imagery, elevation, erosion observation, and climate data. Regular interannual data collection can alleviate this challenge for future investigations. Meshik's experience highlights the danger posed by major coastal reconfiguration, a phenomenon expected to occur more rapidly in the Arctic with the onset of climate change.

## ACKNOWLEDGMENTS

This research was made possible by funding and support from Alaska Sea Grant (grant NA14OAR4170079, project R/127-01), the Bristol Bay Native Association, the Bureau of Indian Affairs, the Alaska Division of Geological & Geophysical Surveys, the National Science Foundation (OISE-1927553 OPD-1848542), and the Native Village of Port Heiden. We thank the many residents of Port Heiden who shared experiences, collected observations, and always brought a fun and enthusiastic atmosphere. We thank Jaclyn, John, and James Christensen for sharing knowledge, experience, and photographs. We also thank Port Heiden's Tribal Environmental Office staff for providing technical support and collecting year-round field measurements. Finally, we

thank Sue Flensburg, Gabe Dunham, and Mike Brubaker for their tireless efforts supporting Bristol Bay communities.

## LITERATURE CITED

Alaska Rural Water and Sanitation Working Group, 2015. *Alaska Water and Sanitation Retrospective 1970–2005*. Anchorage: U.S. Arctic Research Commission, 22p.

Bacon, C.R.; Neal, C.A.; Miller, T.P.; McGimsey, R.G., and Nye, C.J., 2014. *Postglacial Eruptive History, Geochemistry, and Recent Seismicity of Aniakchak Volcano, Alaska Peninsula*. Reston, Virginia: U.S. Geological Survey, *Professional Paper 1810*, 74p.

Barton, L.; Shirar, S., and Jordan, J.W., 2018. Holocene human occupation of the central Alaska Peninsula. *Radiocarbon*, 60(2), 367–382.

Bromirski, P.D.; Cayan, D.R.; Helly, J., and Wittmann, P., 2013. Wave power variability and trends across the North Pacific. *Journal of Geophysical Research: Oceans*, 118(12), 6329–6348.

Bronen, R. and Chapin, F.S., 2013. Adaptive governance and institutional strategies for climate-induced community relocations in Alaska. *Proceedings of the National Academy of Sciences of the United States of America*, 110(23), 9320–9325.

Bronen, R.; Pollock, D.; Overbeck, J.R.; Stevens, D.; Natali, S., and Maio, C.V., 2020. Usteq: Integrating indigenous knowledge and social and physical sciences to coproduce knowledge and support community-based adaptation. *Polar Geography*, 43(2–3), 188–205.

Buzard, R.M., 2021. *Photogrammetry-Derived Historical Orthoimagery for Homer, Alaska from 1951, 1952, 1964, and 1985*. Fairbanks: Alaska Division of Geological & Geophysical Surveys, *Raw Data File 2021-21*, 10p.

Buzard, R.M.; Glenn, R.J.T.; Miller, K.Y., and Overbeck, J.R., 2021a. *Photogrammetry-Derived Orthoimagery and Elevation for Goldfish Lake in Port Heiden, Alaska, Collected May 7, 2021*. Fairbanks: Alaska Division of Geological & Geophysical Surveys, *Raw Data File 2021-19*, 4p.

Buzard, R.M.; Overbeck, J.R.; Chriest, J.; Endres, K.L., and Plumb, E.W., 2021b. *Coastal Flood Impact Assessments for Alaska Communities*. Fairbanks, Alaska: Alaska Division of Geological & Geophysical Surveys, *Report of Investigation 2021-01*, 16p.

Buzard, R.M.; Turner, M.M.; Miller, K.Y.; Antrobus, D.C., and Overbeck, J.R., 2021c. *Erosion Exposure Assessment of Infrastructure in Alaska Coastal Communities*. Fairbanks, Alaska: Alaska Division of Geological & Geophysical Surveys, *Report of Investigation 2021-03*, 29p.

Davis, R.A., 1994. Barrier island systems—A geologic overview. In: Davis, R.A. (ed.), *Geology of Holocene Barrier Island Systems*. Berlin: Springer, pp. 1–46.

Davis, R.A., Jr., and Hayes, M.O., 1984. What is a wave-dominated coast? *Marine Geology*, 60(1–4), 313–329.

DeGrandpre, K.G. and Freymueller, J.T., 2019. Vertical velocities, glacial isostatic adjustment, and earth structure of northern and western Alaska based on repeat GPS measurements. *Journal of Geophysical Research: Solid Earth*, 124, 9148–9163.

Detterman, R.L.; Miller, T.P.; Yount, M.E., and Wilson, F.H., 1981. *Quaternary Geologic Map of the Chignik and Sutuik Island Quadrangles, Alaska*. Fairbanks, Alaska: U.S. Geological Survey, *Miscellaneous Investigations Series Map 1292*, scale 1:250,000, 1 sheet.

Farquharson, L.M.; Mann, D.H.; Swanson, D.K.; Jones, B.M.; Buzard, R.M., and Jordan, J.W., 2018. Temporal and spatial variability in coastline response to declining sea-ice in northwest Alaska. *Marine Geology*, 404, 71–83.

Fathauer, T.F., 1978. *A Forecast Procedure for Coastal Floods in Alaska*. Anchorage, Alaska: NOAA, *Technical Memorandum NWS AR-23*, 27p.

FitzGerald, D.M.; Hein, C.J.; Hughes, Z.; Kulp, M.; Georgiou, I., and Miner, M., 2018. Runaway barrier island transgression concept: Global case studies. In: Moore, L.J. and Murray, A.B. (eds.), *Barrier Dynamics and Response to Changing Climate*. Cham, Switzerland: Springer, pp. 3–56.

Fritz, M.; Vonk, J.E., and Lantuit, H., 2017. Collapsing Arctic coastlines. *Nature Climate Change*, 7, 6–7.

Gibbs, A.E. and Richmond, B.M., 2015. *National Assessment of Shoreline Change—Historical Shoreline Change along the North Coast of Alaska, U.S.–Canadian Border to Icy Cape*. Reston, Virginia: U.S. Geological Survey, *Open File Report 2015-1048*, 96p.

Hartmann, B. and Wendler, G., 2005. The significance of the 1976 Pacific climate shift in the climatology of Alaska. *Journal of Climate*, 18, 4824–4839.

Hayes, M.O., 1979. Barrier island morphology as a function of tidal and wave regime. In: Leatherman, S.P. (ed.), *Barrier Islands from the Gulf of St. Lawrence to the Gulf of Mexico*. Cambridge, Massachusetts: Academic Press, pp. 1–28.

Hersbach, H.; Bell, B.; Berrisford, P.; Hirahara, S.; Horányi, A.; Muñoz-Sabater, J.; Nicolas, J.; Peubey, C.; Radu, R.; Schepers, D.; Simmons, A.; Soci, C.; Abdalla, S.; Abellán, X.; Balsamo, G.; Bechtold, P.; Biavati, G.; Bidlot, J.; Bonavita, M.; Chiara, G.; Dahlgren, P.; Dee, D.; Diamantakis, M.; Dragani, R.; Flemming, J.; Forbes, R.; Fuentes, M.; Geer, A.; Haimberger, L.; Healy, S.; Hogan, R.J.; Hólm, E.; Janisková, M.; Keeley, S.; Laloyaux, P.; Lopez, P.; Lupu, C.; Radnoti, G.; Rosnay, P.; Rozum, I.; Vamborg, F.; Villaume, S., and Thépaut, J., 2020. The ERA5 global reanalysis. *Quarterly Journal of the Royal Meteorological Society*, 146, 1999–2049.

Himmelstoss, E.A.; Henderson, R.E.; Kratzmann, M.G., and Farris, A.S., 2018. *Digital Shoreline Analysis System (DSAS) Version 5.0 User Guide*. Reston, Virginia: U.S. Geological Survey, *Open-File Report 2018-1179*, 110p.

Hubbard, B.R., 1952. *Alaskan Odyssey*. London: Robert Hale, 198p.

Hunter, R.E.; Sallenger, A.H., and Dupre, W.R., 1979. *Maps Showing Directions of Longshore Sediment Transport along the Alaskan Bering Sea Coast*. Fairbanks, Alaska: U.S. Geological Survey, *Miscellaneous Field Studies Map 1049*, 7p, scale 1:400,000, 5 sheets.

Iliaska Environmental Staff, 2008. *Phase I Environmental Site Assessment at the Meshik Town Site near Port Heiden, Alaska*. Homer, Alaska: Iliaska Environmental, 45p.

Irrgang, A.M.; Bendixen, M.; Farquharson, L.M.; Baranskaya, A.V.; Erikson, L.H.; Gibbs, A.E.; Ogorodov, S.A.; Overduin, P.P.; Lantuit, H.; Grigoriev, M.N., and Jones, B.M., 2022. Drivers, dynamics and impacts of changing Arctic coasts. *Nature Reviews Earth & Environment*, 3(1), 39–54.

Jones, B.M.; Farquharson, L.M.; Baughman, C.A.; Buzard, R.M.; Arp, C.D.; Grosse, G.; Bull, D.L.; Günther, F.; Nitze, I.; Urban, F.; Kasper, J.L.; Frederick, J.M.; Thomas, M.; Jones, C.; Mota, A.; Dallimore, S.; Tweedie, C.; Maio, C.; Mann, D.H.; Richmond, B.; Gibbs, A.; Xiao, M.; Sachs, T.; Iwahana, G.; Kanevskiy, M., and Romanovsky, V.E., 2018. A decade of remotely sensed observations highlight complex processes linked to coastal permafrost bluff erosion in the Arctic. *Environmental Research Letters*, 13. doi: 10.1088/1748-9326/aae471

Jordan, J.W., 2001. Late Quaternary sea level change in Southern Beringia: Postglacial emergence of the Western Alaska Peninsula. *Quaternary Science Reviews*, 20(1–3), 509–523.

Kaufman, D.S. and Manley, W.F., 2004. Pleistocene Maximum and Late Wisconsinan glacier extents across Alaska, USA. In: Ehlers, J. and Gibbard, P.L. (eds.), *Quaternary Glaciations—Extent and Chronology, Part II, North America*. Amsterdam: Elsevier, pp. 9–27.

Khouodobine, M., 1828. *Carte de la Côte Septentr de la Presqu ile d'Alaska sur les Relievemens Pris de la Corvette Moller [Map of the Northern Coast of the Alaska Peninsula on the Reliefs Taken from the Corvette Moller]*. 1 sheet.

Kvasager, D.W., 1975. *Erosion Study for Port Heiden, Alaska*. Anchorage: Hewitt V. Lounsbury & Associates, 14p.

Legare, H., 2000. *Field Trip to Port Heiden (Memorandum)*. Elmendorf Air Force Base, Alaska: U.S. Army Corps of Engineers, Hydraulic and Hydrology Section, 11p.

Lewis, J.F., 1867. *Map of Russian America or Alaska Territory: Compiled from Russian Charts and Surveys by Col. C.E. Bulkley*. 1 sheet.

Leonardi, N.; Ganju, N.K., and Fagherazzi, S., 2016. A linear relationship between wave power and erosion determines salt-

marsh resilience to violent storms and hurricanes. *Proceedings of the National Academy of Sciences*, 113(1), 64–68.

Lujan, E.; Brubaker, M.; Warren, J.; Christensen, J.; Anderson, S.; O'Domin, M.; Littell, J.S.; Buzard, R.M.; Overbeck, J.R.; Holen, D.; Flensburg, S., and Powers, E., 2018. *Climate Change in Port Heiden, Alaska: Strategies for Community Health*. Anchorage: Alaska Native Tribal Health Consortium, 51p.

Mantua, N.J. and Hare, S.R., 2002. The Pacific decadal oscillation. *Journal of Oceanography*, 58, 35–44.

Mason, O.K.; Salmon, D.K., and Ludwig, S.L., 1996. The periodicity of storm surges in the Bering Sea from 1898 to 1993, based on newspaper accounts. *Climate Change*, 34, 109–123.

McCabe, G.J.; Clark, M.P., and Serreze, M.C., 2001. Trends in northern hemisphere surface cyclone frequency and intensity. *Journal of Climate*, 14, 2763–2768.

Mesquita, M.D.S.; Atkinson, D.E., and Hodges, K.I., 2010. Characteristics and variability of storm tracks in the North Pacific, Bering Sea, and Alaska. *Journal of Climate*, 23, 294–311.

Morseth, M., 2003. *Puyulek pu'irtuq! The People of the Volcanoes*. Anchorage: National Park Service, 207p.

Mulhern, J.S.; Johnson, C.L., and Martin, J.M., 2017. Is barrier island morphology a function of tidal and wave regime? *Marine Geology*, 387, 74–84.

Nienhuis, J.H. and Lorenzo-Trueba, J., 2019. Can barrier islands survive sea-level rise? Quantifying the relative role of tidal inlets and overwash deposition. *Geophysical Research Letters*, 46, 14,613–14,621.

NOAA (National Oceanic and Atmospheric Administration), 2003. *Computational Techniques for Tidal Datums Handbook*. Silver Spring, Maryland: National Oceanic and Atmospheric Administration, NOAA Special Publication No. NOS CO-OPS 2, 98p.

NOAA, 2015. *NOAA Nautical Chart 16343: Port Heiden*. Silver Spring, Maryland: U.S. Department of Commerce, scale 1:80,000, 1 sheet.

Overbeck, J.R.; Buzard, R.M., and Maio, C.V., 2017. Storm impacts in western Alaska: Documenting shoreline change and flooding through remote sensing and community-based monitoring. *Proceedings of the OCEANS 2017 Anchorage Conference* (Anchorage), pp. 684–689.

Overbeck, J.R.; Buzard, R.M.; Turner, M.M.; Miller, K.Y., and Glenn, R.J., 2020. *Shoreline Change at Alaska Coastal Communities*. Anchorage, Alaska: Alaska Division of Geological & Geophysical Surveys, *Report of Investigation 2020-10*, 35p, 43 sheets.

Overeem, I.; Anderson, R.S.; Wobus, C.W.; Clow, G.D.; Urban, F.E., and Matell, N., 2011. Sea ice loss enhances wave action at the Arctic coast. *Geophysical Research Letters*, 38(L17503), 1–6.

Pease, C.H.; Schoenberg, S.A., and Overland, J.E., 1982. *A Climatology of the Bering Sea and Its Relation to Sea Ice Extent*. Seattle: NOAA, Technical Report ERL 419-PMEI 36, 29p.

Pollard, J.A.; Christie, E.K.; Spencer, T., and Brooks, S.M., 2022. Gravel barrier resilience to future sea level rise and storms. *Marine Geology*, 444, 1–16.

Reimnitz, E., 1990. A review of beach nourishment from ice transport of shoreface materials, Beaufort Sea, Alaska. *Journal of Coastal Research*, 6(2), 439–470.

Ringsmuth, K.J., 2007. *Beyond the Moon Crater Myth: A New History of the Aniakchak Landscape*. Anchorage: National Park Service, 262p.

Rodionov, S.N.; Bond, N.A., and Overland, J.E., 2007. The Aleutian Low, storm tracks, and winter climate variability in the Bering Sea. *Deep Sea Research Part II*, 54, 2560–2577.

Sallenger, A.H., Jr., and Hunter, R.E., 1984. *Maps Showing the Coastal Morphology of the Bristol Bay Coast of the Alaska Peninsula*. Fairbanks, Alaska: U.S. Geological Survey, *Miscellaneous Field Studies Map 1672*, scale 1:400,000, 2 sheets.

Schwing, E., 2022. A massive storm destroyed fishing boats in Alaska, leading to fears of food insecurity. *NPR KTOO*, 25 September. <https://www.npr.org/2022/09/25/1124974251/a-massive-storm-destroyed-fishing-boats-in-alaska-leading-to-fears-of-food-insec>

ShoreZone, 2022. *ShoreZone Shore Types and Photos of Alaska*. <http://shorezone.org>

Smith, W.R. and Baker, A.A., 1924. *Mineral Resources of Alaska, Report on Progress of Investigations in 1922: The Cold Bay-Chignik District, Alaska*. Washington, D.C.: U.S. Geological Survey, *Bulletin 755*, pp. 151–222, scale 1:792,000, 1 sheet.

Stergiou, E., 2013. *Coastal Impact Assistance Program Waste Erosion Assessment and Review Trip Report*. Anchorage: Alaska Department of Environmental Conservation, 5p.

Stutz, M.L. and Pilkey, O.H., 2011. Open-ocean barrier islands: Global influence of climatic, oceanographic, and depositional settings. *Journal of Coastal Research*, 27(2), 207–222.

Terzeni, J.; Jorgenson, M.T., and Ely, C.R., 2014. Storm-surge flooding on the Yukon–Kuskokwim Delta, Alaska. *Arctic*, 67(3), 360–374.

U.S. Coast and Geodetic Survey, 1944. *Alaska Peninsula and Aleutian Islands to Seguam Pass*. Washington, D.C.: U.S. Coast and Geodetic Survey (USCGS), USCGS 8802, scale 1:1,023,188, 1 sheet.

U.S. Commission of Fish and Fisheries, 1888. *Aliaska Peninsula and Adjacent Islands. Report on Explorations of Alaskan Fishing Grounds*. Buffalo, New York: U.S. Commission of Fish and Fisheries, scale 1:1,150,000, 1 sheet.

U.S. Geological Survey, 1963. *Quadrangle for Chignik D-3, AK*. Fairbanks, Alaska: U.S. Geological Survey, scale 1:63,360, 1 sheet.

U.S. Government Accountability Office Staff, 2022. *Alaska Native Issues: Federal Agencies Could Enhance Support for Native Village Efforts to Address Environmental Threats*. U.S. Washington, D.C.: Government Accountability Office, GAO-22-104241, 96p.

U.S. Weather Bureau, 1957. *Climatological Data: March 1957*. Asheville, North Carolina: U.S. Department of Commerce, 8(3), 49p.

USACE (U.S. Army Corps of Engineers), 2009. *Alaska Baseline Erosion Assessment: Study Findings and Technical Report*. Elmendorf Air Force Base, Alaska: USACE Alaska District, 65p.

Vermaire, J.C.; Pisaric, M.F.J.; Thienpont, J.R.; Courtney Mustaphi, C.J.; Kokelj, S.V., and Smol, J.P., 2013. Arctic climate warming and sea ice declines lead to increased storm surge activity. *Geophysical Research Letters*, 40, 1386–1390.

Vitousek, S.; Barnard, P.L.; Fletcher, C.H.; Frazer, N.; Erikson, L., and Storlazzi, C.D., 2017. Doubling of coastal flooding frequency within decades due to sea-level rise. *Scientific Reports*, 7, 1399.

Walsh, J.E.; Fetterer, F.; Stewart, J.S., and Chapman, W.L., 2017. A database for depicting Arctic sea ice variations back to 1850. *Geographical Review*, 107(1), 89–107.

Walsh, J.E. and Johnson, C.M., 1979. An analysis of Arctic sea ice fluctuations, 1953–77. *Journal of Physical Oceanography*, 9, 580–591.

Wang, J.; Kim, H.M., and Chang, E.K.M., 2017. Changes in northern hemisphere winter storm tracks under the background of arctic amplification. *Journal of Climate*, 30, 3705–3724.

Yadav, J.; Kumar, A., and Mohan, R., 2020. Dramatic decline of Arctic sea ice linked to global warming. *Natural Hazards*, 103(2), 2617–2621.